

# An Application of Damped Diffusion for Modeling Volatility Dynamics

Mao-Wei Hung<sup>1</sup>, Yi-Chen Ko <sup>2</sup> and Jr-Yan Wang<sup>3</sup>

<sup>1</sup>National Taiwan University, <sup>2</sup>National Taiwan University and <sup>3</sup>National Taiwan University

Address correspondence to Yi-Chen Ko, National Taiwan University, No. 1, Sec. 4, Roosevelt Road, Taipei 10617, Taiwan, or e-mail: d97724012@ntu.edu.tw.

Received March 20, 2020; revised March 14, 2021; editorial decision June 21, 2021; accepted June 29, 2021

## Abstract

This paper proposes a damped constant elasticity variance (CEV) stochastic volatility (DCEV) model, which remedies the possible explosive behavior of the CEV model and also accommodates the mean-reverting dynamics more appropriately than the nonlinear drift (NLD) stochastic volatility model. As the DCEV model maintains the linear drift, an analytic formula is available to efficiently infer latent variances from VIX levels, after which both its physical and risk-neutral parameters can be simultaneously estimated with the maximum-likelihood approach given S&P 500 returns and inferred variances. The DCEV model outperforms the CEV and NLD models in in-sample fitting performance and in out-of-sample variance forecasting under the physical measure. It also exhibits superior ability in out-of-sample option pricing over the CEV and [Heston's \(1993\)](#) models under the risk-neutral measure. This satisfactory performance demonstrates the suitability of describing volatility dynamics with the DCEV model and the potential of applying this to study other issues.

**Key words:** constant elasticity variance (CEV), damping function, linear drift, nonaffine stochastic volatility model, nonlinear drift

**JEL classification:** G10, G13

Since volatility dynamics are critical in derivative pricing, risk management, and even asset allocation, there is a growing literature investigating the empirical performance of the stochastic volatility (SV) model. According to [Duffie, Pan, and Singleton \(2000\)](#), an affine jump-diffusion model (hereafter termed simply “affine model”) is defined such that the drift vector, instantaneous covariance matrix, and jump intensities all have affine dependence on the state vector. Under this framework, analytical tractability can be attained for a wide variety of valuation and estimation problems. One of the most classical affine SV models is [Heston's \(1993\)](#) square root (SQR) SV model, which considers the SQR of variance in the diffusion part of the proposed SV model to account for time-varying volatility and the leverage effect. However, an empirical consensus has gradually formed that the SQR model is insufficient to

describe the dynamics of equity returns. As a result, this paper—along with abundant literature—focuses on exploring a more appropriate SV model to fit empirical data.

By maintaining the affine property, [Bates \(1996\)](#) proposes an SQR model augmented with price jumps and finds it captures the possibility of discontinuities in the stock price dynamic. [Bakshi, Cao, and Chen \(1997\)](#) show that the inclusion of price jumps in the SQR model has little effect on pricing and hedging longer-maturity S&P500 index options, but worsens the hedging performance for shorter-maturity options. [Bates \(2000\)](#) evaluates the performance of the two-SQR SV model with price jumps on pricing S&P 500 futures options and concludes that price jumps are necessary even with an additional volatility factor. [Pan \(2002\)](#) adopts the SQR model with price jumps to price S&P 500 index options and finds that jump specification is important in explaining time-varying volatility smiles. [Eraker, Johannes, and Polson \(2003\)](#) study an SQR model with contemporaneous jumps in price and volatility dynamics and conclude that the proposed model improves fitting performance on the S&P 500 index price. However, exploiting the similar model specification of [Eraker, Johannes, and Polson \(2003\)](#), [Eraker \(2004\)](#) argues that jumps have little or no effect on pricing S&P 500 index options. [Broadie, Chernov, and Johannes \(2007\)](#), by contrast, find strong evidence of improvement from introducing price and volatility jumps into the SQR model for pricing S&P 500 futures options. The impacts from introducing jumps in affine SV models are mixed, which implies the actual source of problems may arise from the affine specification of SV models.

In order to capture richer volatility structures, research has been conducted on nonaffine SV models with more flexible drift or diffusion functions that can be incorporated to match higher-moment statistics observed in actual data. There are two major categories of nonaffine SV models. The first exploits the concept of the constant elasticity of variance to model the diffusion part in an SV model [called a constant elasticity variance (CEV) model hereafter]. [Ait-Sahalia and Kimmel \(2007\)](#) examine the fitting performance of a CEV model for the S&P 500 and VIX indices and argue that the SQR model is misspecified. [Duan and Yeh \(2010\)](#) estimate a jump-diffusion CEV model with spot prices and theoretical volatility levels, which are analytically transformed from VIX index values. They conclude that the CEV model outperforms the SQR model even with the existence of jumps. For modeling the S&P 100 index, [Jones \(2003\)](#) proposes an extended CEV model with two CEV components, one (the other) of which is perfectly correlated with (independent from) the spot Brownian motion. His empirical results suggest that the proposed model exhibits better explaining power for price returns than a jump-diffusion SQR model. [Kaeck and Alexander \(2012\)](#) also propose a CEV model with a stochastic long-run volatility mean and contemporaneous jumps in both spot and volatility to fit the S&P 500 and VIX indices; they find that either the CEV model or GARCH (generalized autoregressive conditional heteroskedasticity) model (with a unity exponent term for the CEV diffusion) outperforms the SQR model.

The second category of nonaffine SV models replaces the mean-reverting linear drift (LD) with a more general non-linear drift in an SV model (NLD model henceforth). Unless otherwise specified, the NLD model discussed in this paper follows [Ait-Sahalia's \(1996\)](#) NLD interest rate model to formulate the drift term as  $(\alpha_0 + \alpha_1 X_t + \alpha_2 X_t^2 + \alpha_3 X_t^{-1})$ <sup>1</sup> and

1 Other NLD literature may consider a less generally quadratic drift term, such as [Ahn and Gao \(1999\)](#) and [Christoffersen, Jacob, and Mimouni \(2010\)](#). In addition to the NLD and CEV models, a stochastic log volatility model is studied in [Durham \(2007, 2013\)](#) and [Ferriani and Pastorello \(2012\)](#).

the diffusion term as a CEV variance of  $\sigma X_t^2$ , where  $X_t$  denotes the value of the state variable. The restrictions of  $\alpha_2 < 0$  and  $\alpha_3 > 0$ , respectively, capture reversals in the drift at the high and low ends of the spectrum of the state variable. Generally speaking, the mean-reverting property of the NLD method is reinforced near both ends, compared with the LD model. Bakshi, Ju, and Ou-Yang (2006) test the fitting performance of the NLD model by directly taking the VXO index as the proxy of volatility and find that the NLD model outperforms LD-based affine and nonaffine models. Moreover, the investigations of the S&P 500 and VIX indices in Christoffersen, Jacob, and Mimouni (2010), the VIX index and realized volatility in Chourdakis and Dotsis (2011), the S&P 500 index in Ignatieva, Rodrigues, and Seeger (2015), and the S&P 100 and VXO indices in Mijatovic and Schneider (2014) are also employed to examine the importance of NLD for volatility dynamics. All of the above-mentioned SV models are summarized and classified in Table 1.

This paper differs in that it is the first time a damping function has been used to formulate the diffusion part of the SV model. Instead of combining the NLD and CEV models, we maintain the LD and follow Li (2010)<sup>2</sup> in introducing a damped superimposed CEV diffusion into an SV model (henceforth termed the DCEV model). There are several potential merits regarding this specification. First of all, due to the appealing LD property, our DCEV model has a closed-form solution for the expected volatility, which is a desired quantity in many applications and more importantly helpful for us to efficiently extract latent volatility values from prevailing VIX levels. Second, the DCEV model may be more appropriate for describing the mean-reverting property when the value of the state variable is near its high and low ends. When the value of the state variable is high, the damping function and thus the diffusion term approaches zero. Consequently, interference from the diffusion term is minimized such that the downward mean-reverting force from the LD is effectively pronounced, which is analogous to the effect of  $\alpha_2 X_t^2$  for  $\alpha_2 < 0$  in the NLD model to enhance the mean-reverting force when the state variable is high. When the value of the state variable is low, the term  $\alpha_3 X_t^{-1}$  for  $\alpha_3 > 0$  in the NLD model represents an extremely strong mean-reverting force (due to the singularity point at the lower-end value of the state variable) to pull up the value of the state variable. However, this force is not necessarily observed in the real world. For a market experiencing a calm period, it is possible to observe a volatility that remains low for a while, but an NLD with the term of  $\alpha_3 X_t^{-1}$  ( $\alpha_3 > 0$ ) almost eliminates this possibility. Finally, pure CEV diffusion could lead to difficulty in estimation for exponent terms significantly greater than 1, which could result in an explosive scenario for some high levels of the state variable. In contrast, the DCEV model eliminates this possibly explosive behavior by governing the effective variants of CEV diffusion for high state variable values. These merits motivate us to employ the DCEV model to capture SV dynamics. To the best of our knowledge, this paper is the first to propose and empirically examine a DCEV model for SV.

Note that in this paper we do not account for the jump feature, because we believe that the choice of an appropriate volatility dynamic is far more important than the inclusion of

- 2 Li (2010) is the first to apply the DCEV model to formulate the stochastic interest rate process. He suggests that a more appropriate diffusion function may be more valuable than the NLD model, because the DCEV stochastic interest rate model outperforms Ait-Sahalia's (1996) NLD stochastic interest rate model for 1963–1998 federal funds rates, even though the DCEV model has fewer parameters than the NLD model.

**Table 1** Classification of SV models

Information sets for estimation	Affine SV model	Nonaffine SV model
S	Eraker, Johannes, and Polson (2003), SQR_CJ	Chacko and Viceira (2003), CEV_J; Chernov et al. (2003), CEV_CJ; Ignatieva, Rodrigues, and Seeger (2015), NLD_CJ
V		Bakshi, Ju, and Ou-Yang (2006), NLD; Chourdakis and Dotsis (2011), NLD
Option	Heston (1993), SQR; Bates (1996, 2000), SQR_J; Bakshi, Cao, and Chen (1997), SQR_J; Pan (2002), SQR_J; Broadie, Chernov, and Johannes (2007), SQR_CJ	
S and Option	Eraker (2004), SQR_CJ	Christoffersen, Jacob, and Mimouni (2010), NLD_J
S and V		Jones (2003), CEV; Ait-Sahalia and Kimmel (2007), CEV; Duan and Yeh (2010), CEV_J; Kaeck and Alexander (2012), CEV_CJ; Mijatovic and Schneider (2014), NLD; Proposed model: DCEV

*Notes:* This table classifies SV models according to their affine or nonaffine property and different information sets used for estimation. The “S” or “V” sets, respectively, correspond to estimation using series of spot prices or realized (or inferred) volatilities. “SQR” indicates the SQR SV model specified in Heston (1993). “J” or “CJ,” respectively, represent spot price jumps or contemporaneous jumps in spot and volatility. “NLD” and “CEV” indicate a non-linear drift term [in Ait-Sahalia’s (1996) form] and constant elasticity of variance diffusion, respectively. Except for Bakshi, Ju, and Ou-Yang (2006) and Mijatovic and Schneider (2014), the NLD models discussed here are all accompanied with the CEV diffusion term. Bakshi, Ju, and Ou-Yang (2006) use a diffusion function in the form of  $\sqrt{\beta_0 + \beta_1 V_t + \beta_2 \bar{V}_t}$ , and Mijatovic and Schneider (2014) adopt a GARCH-type diffusion term by fixing the exponent of the CEV diffusion to be unity. For non-NLD models, they follow the same LD term as that in Heston (1993).

jumps in spot prices or volatilities. The same argument can be found in Jones (2003) and Kaeck and Alexander (2012).<sup>3</sup> In fact, as long as one first identifies a best-performing SV

3 Recent literature which examines SV models by testing the pricing performance for VIX derivatives also supports this argument. For example, Branger, Kraftschika, and Volkerta (2016) find that the most important factor to include in a variance process is a stochastic mean-reversion long-term mean, followed by a stochastic volatility of volatility, and finally followed by variance jumps. In Lo et al. (2019), they find that it is always useful to include the second variance component. When examining short-term (shorter than 60 days) contracts, the improved performance for introducing variance jumps is comparable to that of introducing the second variance component. Only when examining long-term (longer than 180 days) contracts, incorporating the variance jump in the

model with the absence of jumps, adding jumps in spot price or volatility processes definitely may enhance the in-sample fitting performance in most cases. Meanwhile, it is not rare to find that the out-of-sample forecasting power is not improved after the inclusion of jumps, see [Kaeck and Alexander \(2012\)](#) for example. We note that the inclusion of jumps may cause problems with overfitting, and the question of whether infrequent jumps occur in out-of-sample data may affect significantly the out-of-sample performance of an SV model with jumps. To avoid unexpected issues caused by jumps, this paper focuses on investigating the best-performing SV dynamic without jumps.

To estimate our DCEV model, we employ both the series of spot prices and inferred variances due to several reasons. First, a relatively long sample period is needed to obtain reliable estimations if using only the series of spot prices, since the instantaneous variance is nonobservable and its effect is hidden in the series of spot prices. Second, employing individual spot price or volatility time series for estimation disregards the correlation between them, but the negative correlation between the asset price and its volatility is an important and unneglectable feature for various financial issues. Third, option data allow the accurate estimation of latent volatility because volatility is an important factor in determining the option price. However, with approaches using only option-implied volatilities, it is difficult to estimate physical-measure parameters (i.e., parameter values in the real world) and determine their statistic inferences. Due to these concerns, there is a growing stream of literature exploiting both spot returns and derivatives (such as options or volatility proxies) to estimate SV models. This paper also adopts this type of estimation method. To be more specific, we follow [Jones \(2003\)](#), [Ait-Sahalia and Kimmel \(2007\)](#), [Duan and Yeh \(2010\)](#), [Kaeck and Alexander \(2012\)](#), and [Mijatovic and Schneider \(2014\)](#) to estimate the series of latent volatilities and then employ both the series of logarithmic spot returns and inferred variances to simultaneously estimate the physical and risk-neutral parameters for the proposed model. In addition to distinguishing affine or nonaffine SV models, in [Table 1](#) we also categorize SV models according to the information sets used for estimation. The proposed DCEV model and the estimation method utilized in this paper belong to the category on the lowest right block.

Since volatility is nonobservable, several methods have been proposed to extract volatility levels from other asset prices. [Bakshi, Ju, and Ou-Yang \(2006\)](#) simply use volatility indexes as proxies for latent volatility levels, although they should not be the same theoretically. [Bates \(1996, 2000\)](#); [Bakshi, Cao, and Chen \(1997\)](#); [Pan \(2002\)](#); and [Broadie, Chernov, and Johannes \(2007\)](#) obtain implied volatilities by calibrating option data. [Chernov et al. \(2003\)](#); [Eraker, Johannes, and Polson \(2003\)](#); and [Ignatieva, Rodrigues, and Seeger \(2015\)](#) employ simulation approaches to infer latent volatility levels solely based on stock price data. However, calibrating options and simulation approaches are both time-consuming. Utilizing a suitable volatility proxy is clearly a more efficient method. [Duan and Yeh \(2010\)](#) propose an efficient approach to extract instantaneous volatility levels of the S&P 500 index given observations of the VIX index. Due to the fact that the latent volatility level can be expressed as a function of VIX, [Duan and Yeh \(2010\)](#) propose an analytic

variance component with a lower mean-reversion speed does further improve the pricing fit given the presence of the second variance component.

transformation between the two by exploiting the LD property.<sup>4</sup> Once the volatility level can be inferred, [Duan and Yeh \(2010\)](#) discretize the stochastic differential equations using the Euler method and estimate both physical and risk-neutral parameters of their jump-diffusion CEV model by maximizing the likelihood value of the joint density function of spot returns and inferred variances. Many papers have adopted procedures similar to [Duan and Yeh \(2010\)](#) to extract volatility levels but employ methods other than the maximum-likelihood method to estimate the joint density function of spot prices and volatilities, such as the Markov chain Monte Carlo (MCMC) method in [Jones \(2003\)](#) and [Kaeck and Alexander \(2012\)](#), likelihood expansion based on Hermite polynomials in [Ait-Sahalia and Kimmel \(2007\)](#), or expected maximum likelihood in [Mijatovic and Schneider \(2014\)](#). Recall that since this paper takes advantage of the DCEV model rather than the NLD model to govern the volatility mean-reverting behavior, we can thus retain the LD term in DCEV model, which allows us to adopt a similar method to that suggested in [Duan and Yeh \(2010\)](#) to infer volatility levels.

To show the advantages of the proposed DCEV model in estimating both physical and risk-neutral parameters, we conduct several experiments to investigate its in-sample fitting and out-of-sample forecasting performance. The in-sample test evaluates the fitting performance of the DCEV, pure CEV, and NLD models based on daily spot price and VIX index data from 1996 to 2017. As for inferring latent volatility, [Duan and Yeh's \(2010\)](#) analytic transformation approach is utilized for the DCEV and CEV models. Furthermore, to ensure the comparability with the NLD model for which there is no simple translation between the VIX index and the instantaneous volatility, we mimic [Duan and Yeh's \(2010\)](#) transformation form by introducing a data-implied linear relationship to approximately infer latent variance from the squared VIX index for the NLD model. After obtaining inferred variances, all of the examined models can be estimated through the maximum-likelihood method. For the in-sample analyses, the DCEV model always outperforms the competing models in terms of a higher log-likelihood (LL) value, a smaller Akaike information criterion (AIC) or a smaller [Hong and Li's \(2005\)](#)  $Q$ -statistic, which shows that the superior performance of the DCEV model arises from the advanced model specification rather than the inclusion of additional parameters. In the out-of-sample analyses, we consider two experiments: variance forecasting for the realized variance (RV) based on the physical parameters and option pricing for S&P 500 index options based on the risk-neutral parameters. Empirical results indicate that the DCEV model demonstrates a superior ability in forecasting future volatilities and pricing option contracts in almost all cases in terms of its smaller squared forecasting and pricing errors.

4 It is worth noting that for NLD models, one can still express the latent volatility level as a function of VIX, but the analytic transformation is unavailable and numerical methods must be used to infer volatilities from VIX. To the best of our knowledge, [Chourdakis and Dotsis \(2011\)](#) are the only ones to propose a Markov-chain approximation method to numerically transform the VIX to the latent volatility for an SV model with [Ait-Sahalia's \(1996\)](#) NLD specification. Their method is complicated to implement; also, since the drift and diffusion terms are functions of the latent volatility, the assumption that transition probabilities fall within  $[0,1]$  may not hold for all parameter values or volatility levels.

The paper is organized as follows. Section 1 details the proposed DCEV model and estimation method. The dataset and empirical results are reported in Section 2. We conclude the paper in Section 3.

### 1 DCEV Model and Estimation Method

In the proposed DCEV model, the dynamics of the spot price ( $S_t$ ) and its variance ( $V_t$ ) satisfy the following stochastic differential equations under the physical measure:

$$\begin{aligned}
 d\ln S_t &= (\mu - q - 0.5V_t)dt + \sqrt{V_t}dW_t^S, \\
 dV_t &= \kappa^P(\theta^P - V_t)dt + [\sigma_1 V_t^{0.5}D_1(V_t) + \sigma_2 V_t^\gamma D_2(V_t)]dW_t^V,
 \end{aligned}
 \tag{1}$$

where  $\mu$  is the instantaneous expected growth rate;  $q$  is the dividend yield;  $\kappa^P$  is the speed of mean reversion;  $\theta^P$  is the long-run variance level;  $\sigma_1, \sigma_2,$  and  $\gamma$  are the parameters of the CEV-style diffusion terms of the variance process;  $D_i(V_t)$ , for  $i = 1, 2,$  are two continuously differentiable damping functions; and  $W_t^S$  and  $W_t^V$  are two standard Brownian motions with a correlation  $\rho$ . Following Li (2010), we consider the exponential-form damping functions as  $D_1(V_t) = D_2(V_t) = e^{-8V_t^\gamma}$ . Under this setting, the damping function as well as the diffusion part in Equation (1) approaches zero when  $V_t$  is high. Consequently, the effect of the downward mean-reverting force from the LD becomes more pronounced due to the absence of interference from the diffusion parts. When the value of  $V_t$  is low, the damping functions approach unity and the proposed DCEV model behaves like an extended CEV model. Equation (1) is a general SV model that nests many classical affine or nonaffine SV models in the literature as special cases; these include the SQR, CEV, GARCH, and 3/2 (fixes the exponent term of a CEV model to 1.5) models. All nested models based on Equation (1) are summarized in Table 2.

To express the VIX level as a function of the nonobservable  $V_t$ , we follow the standard martingale pricing approach in Duan and Yeh (2010). Under the risk-neutral measure, the system corresponding to Equation (1) becomes

$$\begin{aligned}
 d\ln S_t &= (r - q - 0.5V_t)dt + \sqrt{V_t}d\tilde{W}_t^S, \\
 dV_t &= \kappa(\theta - V_t)dt + [\sigma_1 V_t^{0.5}D_1(V_t) + \sigma_2 V_t^\gamma D_2(V_t)]d\tilde{W}_t^V,
 \end{aligned}
 \tag{2}$$

where  $r$  is the risk-free rate,  $\kappa = \kappa^P + \delta_V$ ,  $\theta = \kappa^P\theta^P / (\kappa^P + \delta_V)$ ,  $\delta_V$  represents the market price of volatility risk, and  $\tilde{W}_t^S$  and  $\tilde{W}_t^V$  are two standard Brownian motions under the risk-neutral measure with a correlation  $\rho$ . Following Duan and Yeh (2010), the squared VIX at time  $t$  equals the expected risk-neutral integrated variance over the future horizon  $\tau = 21/252$ :

$$\text{VIX}_t^2 = \frac{1}{\tau} \int_t^{t+\tau} E_t^Q(V_u)du,
 \tag{3}$$

where  $E_t^Q(\cdot)$  represents the expected value at time  $t$  under the risk-neutral measure  $Q$ . As long as the drift function in Equation (2) is a linear function of  $V_t$ , Equation (3) can be evaluated as

**Table 2** Nested SV models of proposed DCEV model

Model	$\gamma$	$D_1(V_t)$	$D_2(V_t)$
DCEV	Free	$e^{-8V_t^4}$	$e^{-8V_t^4}$
CEV	Free	0	1
3/2	3/2	0	1
GARCH	1	0	1
SQR	1/2	1	0

Note: Parameter settings for the nested SV models of the proposed DCEV model.

$$\text{VIX}_t^2 = \frac{1}{\tau} \int_t^{t+\tau} [V_t e^{-\kappa u} + \theta(1 - e^{-\kappa u})] du,$$

which results in the following  $V_t$ - $\text{VIX}_t^2$  linear relationship whose intercept and slope are functions of  $\kappa^P$ ,  $\theta^P$ ,  $\kappa$ , and  $\tau$ :

$$V_t = \frac{\kappa^P \theta^P}{\kappa} \left( 1 - \frac{\kappa \tau}{1 - e^{-\kappa \tau}} \right) + \frac{\kappa \tau}{1 - e^{-\kappa \tau}} \text{VIX}_t^2. \quad (4)$$

The derivation details of Equation (4) can be found in Duan and Yeh (2010).

### 1.1 In-Sample Estimation Method

To estimate parameters in the stochastic process system of  $(S_t, V_t)$ , we implement a two-step procedure as follows based on both the time series of S&P 500 index prices and VIX indices in the DCEV and CEV models:

Step i. Divide each observation of the VIX level by 100 and then square the result to obtain  $\text{VIX}_t^2$ , the scale of which is thus consistent with  $V_t$ . Next, by exploiting Equation (4), express the latent variance  $V_t$  as a function of  $\text{VIX}_t^2$ ,  $\kappa$  ( $= \kappa^P + \delta_V$ ), and  $\theta$  ( $= \kappa^P \theta^P / (\kappa^P + \delta_V)$ ) such that the parameters  $\kappa^P$ ,  $\theta^P$ , and  $\delta_V$  can be estimated.

Step ii. The Euler discretization method is applied to Equation (1), that is,

$$\ln S_{t+\Delta t} - \ln S_t = (\mu - q - 0.5V_t)\Delta t + \sqrt{V_t \Delta t} \varepsilon_t^S,$$

$$V_{t+\Delta t} - V_t = \kappa^P (\theta^P - V_t) \Delta t + \left[ \sigma_1 V_t^{0.5} D_1(V_t) + \sigma_2 V_t^2 D_2(V_t) \right] \sqrt{\Delta t} \eta_t^V, \quad (5)$$

where  $\eta_t^V = \rho \varepsilon_t^S + \sqrt{1 - \rho^2} \varepsilon_t^V$ ,  $\varepsilon_t^i \sim \text{ND}(0, 1)$  (standard normal distribution) for  $i = S, V$ , and  $\Delta t = 1/252$  (one trading day). Denote the parameter set of the DCEV model as  $\Theta = (\kappa^P, \theta^P, \sigma_1, \sigma_2, \gamma, \rho, \delta_V)$ . The joint density function for  $\ln S_{t+\Delta t}$  and  $V_{t+\Delta t}$  conditional on  $\ln S_t$  and  $V_t$  can be approximated by

$$f(\ln S_{t+\Delta t}, V_{t+\Delta t} | \ln S_t, V_t, \Theta) = \phi_2(\ln S_{t+\Delta t}, V_{t+\Delta t}, \mu_1, \mu_2, \varrho_1^2, \varrho_2^2, \rho) \cdot \Gamma, \quad (6)$$

where  $\Gamma = \kappa \tau / (1 - e^{-\kappa \tau})$  is the Jacobian transformation from  $\text{VIX}_t^2$  to  $V_t$ , and  $\phi_2(\cdot)$  is the bivariate standard normal density function with

$$\mu_1 = \ln S_t + (\mu - q - 0.5V_t)\Delta t,$$



$$\mu_2 = V_t + \kappa^P (\theta^P - V_t) \Delta t,$$

$$\varrho_1 = \sqrt{V_t \Delta t},$$

$$\varrho_2 = \left[ \sigma_1 V_t^{0.5} D_1(V_t) + \sigma_2 V_t^2 D_2(V_t) \right] \sqrt{\Delta t}.$$

Note that the instantaneous expected ex-dividend growth rate,  $\mu - q$ , is estimated by annualizing the arithmetic average of the daily returns during the whole-sample or sub-sample period to avoid possible overidentification for the drift term of the spot price. Finally, we estimate  $\Theta$  by maximizing the LL function:

$$LL = \sum_{t_i} \ln \phi_2(\ln S_{t_i+\Delta t}, V_{t_i+\Delta t}, \mu_1, \mu_2, \varrho_1^2, \varrho_2^2, \rho) + N \ln \left( \frac{\kappa \tau}{1 - e^{-\kappa \tau}} \right), \tag{7}$$

where  $t_i$  for  $i = 0, \dots, N - 1$  represent the examined trading dates and there are a total of  $(N + 1)$  observations of daily data in the estimation period.

For comparison, we also estimate the NLD model. However, the above two-step estimation method is unavailable for the NLD model since there is no simple translation between the VIX index and the latent variance  $V_t$  for the NLD model.<sup>5</sup> To make the NLD and DCEV models comparable, we assume that there is a linear relationship between latent variance  $V_t$  and  $VIX_t^2$  under the NLD model similar to Equation (4), that is,<sup>6</sup>

$$V_t = a + bVIX_t^2 \tag{8}$$

Equipped with Equation (8), the parameters of  $\mu_2$ ,  $\varrho_2$ , and  $\Gamma$  in Equation (6) are replaced with

$$\mu_2 = V_t + \left( \alpha_0 + \alpha_1 V_t + \alpha_2 V_t^2 + \alpha_3 V_t^{-1} \right) \Delta t,$$

- 5 A naive estimation method for the NLD model is to skip Step i by following Bakshi, Ju, and Ouyang's (2006) assumption to simply approximate the latent variance  $V_t$  by the VIX index. Under this setting, we can estimate the NLD model by slightly modifying Step ii as follows. First, Equation (6) is altered by eliminating the second term of the Jacobian transformation. Second, we further revise the variance-related parameters in the bivariate normal density function  $\mu_2$  and  $\varrho_2$  to be the drift and diffusion functions of NLD model. Finally, the parameter set of the NLD model is represented by  $\Theta = (\alpha_0, \alpha_1, \alpha_2, \alpha_3, \sigma, \gamma, \rho)$ . This naive method is also implemented in the previous version of this paper. Since this method does not properly formulate the relationship between the VIX index and instantaneous variance and its fitting performance is inferior to that of the method introduced below, this paper does not report the estimation results of the naive method. However, this part of the estimation results is available from the authors upon request.
- 6 Computational time is the primary reason why we do not employ a brute-force numerical method to evaluate Equation (3) and thus express  $VIX_t^2$  as a function of  $V_t$  for the NLD model. Note that given the required calculation for the double integration, it is already time-consuming to calculate  $VIX_t^2$  numerically based on  $V_t$ , not to mention that one must further numerically solve the latent  $V_t$  based on the observed  $VIX_t$ . Finally, the computational time may increase by several orders of magnitude when the above numerical method is incorporated into our optimization procedure to maximize the likelihood value. Similar arguments are mentioned in Chourdakis and Dotsis (2011).

$$q_2 = \sigma V_t^\gamma \sqrt{\Delta t},$$

$$\Gamma = b.$$

Consequently, the NLD model can be estimated using the same two-step procedure for estimating the DCEV model given its parameter set of  $\Theta = (\alpha_0, \alpha_1, \alpha_2, \alpha_3, \sigma, \gamma, \rho, a, b)$ . It is worth noting that the introduction of Equation (8) is merely a workaround. Since we directly estimate the intercept and slope parameters  $a$  and  $b$ , this transformation method, which is not like Duan and Yeh's (2010) analytic transformation function, does not contain risk-neutral parameters. As a result, the obtained estimation results of the NLD model are purely under the physical measure.

Last, to evaluate the in-sample performance, we utilize the traditional LL and AIC generated by the DCEV, CEV, and NLD models as the criteria. In addition, we also adopt Hong and Li's (2005)  $Q$ -test to examine the appropriateness of model specification as another criterion. Unlike likelihood-based evaluations (such as LL and AIC) which utilize the model-implied conditional density function, the corresponding  $Q$ -statistic is a probability integral transform-based evaluation relying on the model-implied cumulative distribution function, so it provides a different aspect by which to test the in-sample fitting performance of the examined models. However, it requires modifications to accommodate Hong and Li's (2005)  $Q$ -test to examine SV models because the variance time series is actually nonobservable. To account for this, we employ the time series of spot prices to calculate Hong and Li's (2005)  $Q$ -statistic. Specifically, given the estimated parameter values  $\hat{\Theta}$  of an SV model, we first transform  $VIX_t$  into inferred variance  $V_t$  through Equation (4) for the DCEV and CEV models or Equation (8) for the NLD model and then use the transition density of log spot price  $\phi_1\left(\frac{\ln(S_{t+\Delta t}/S_t) - (\mu - q - 0.5V_t)\Delta t}{\sqrt{V_t\Delta t}}\right)$ , where  $\phi_1(\cdot)$  is the univariate standard normal density function, as the fundamental ingredient to compute the  $Q$ -statistic. The details for calculating the  $Q$ -statistics of the examined three SV models are relegated to Appendix A.

## 1.2 Out-of-Sample Analysis Method

In addition to examining the fitting performance of different models, this paper also investigates their out-of-sample forecasting ability, since superior in-sample performance does not necessarily translate to superior performance in out-of-sample periods. We argue that in-sample tests are helpful to learn or identify stylized facts in historical data, but out-of-sample tests for analyzing the actual forecasting power of examined models are indispensable, especially because SV models are always used in a forward-looking way, whether for derivative pricing, risk management, or asset allocation. Therefore, we conduct two experiments to evaluate the out-of-sample performance of the DCEV, CEV, and NLD models, including variance forecasting based on the physical parameters and option pricing based on both the risk-neutral parameters. However, for option pricing, we cannot compare the out-of-sample performance of the NLD models since risk-neutral parameters such as  $\kappa$  and  $\theta$  in Equation (2) cannot be estimated for the NLD model. Instead, the SQR model (Heston SV model) is included for comparison. Another reason for choosing the SQR model is that it is one of the most popular SV models for option pricing in practice due to the existence of the corresponding analytic option pricing formula.

To compare forecasting and actual variance in the out-of-sample tests, we employ the RV as the comparison benchmark, which is commonly used as an unbiased benchmark in *ex post* volatility forecast evaluations and model comparisons as discussed in Andersen, Bollerslev, and Meddahi (2005). The time series of 5-min RV is selected as the proxy of the true variance. The forecasting error is measured by the mean of squared errors (MSEs) of the *D*-day average differences between the variance forecasts of the examined model and the corresponding RVs in different horizons. In addition, a rolling window scheme is adopted in the out-of-sample tests, for which the procedure is described as follows.

To forecast *D*-day-ahead average variance based on model *k* on date *t<sub>i</sub>*,  $FV_{t_i+D}^k$ , where *k* = DCEV, CEV, and NLD, and *D* = 5, 10, and 15, we implement the following five-step procedure:

Step 1. A fixed sample size of the prior 1,000 daily observations, that is, the observations from *t<sub>i-999</sub>* to *t<sub>i</sub>*, are employed to estimate the parameters of different models.

Step 2. We transform  $VIX_{t_i}^2$  to *V<sub>t<sub>i</sub></sub>* using Equation (4) for the DCEV and CEV models and Equation (8) for the NLD model given the parameters estimated in Step 1.

Step 3. To ensure the correct co-varying behavior between the actual innovations of  $\ln S_t$  and the latent volatility for the subsequent *D* days, the particle filter approach suggested by Malik and Pitt (2011) is implemented based on the system of stochastic difference equations in Equation (5). The procedure is summarized below; for details refer to Malik and Pitt (2011):

3.1 We first fix the particles at time *t<sub>i</sub>* as  $V_{t_i}^j = V_{t_i}$  for all *j* = 1, 2, . . . , *M*, where *M* is the number of particles (fixed at 10,000 in this paper) and *V<sub>t<sub>i</sub></sub>* is obtained in Step 2.

3.2 Based on the values of  $\ln S_{t_{i+1}} - \ln S_{t_i}$ , *V<sub>t<sub>i</sub></sub>*, and the parameters from Step 1, the corresponding innovation  $\epsilon_{t_i}^{S,j}$  is derived as

$$\epsilon_{t_i}^{S,j} = \left[ \ln S_{t_{i+1}} - \ln S_{t_i} - \left( \mu - q - 0.5V_{t_i}^j \right) \Delta t \right] / \sqrt{V_{t_i}^j \Delta t}.$$

To obtain the simulated values of the variance at time *t<sub>i+1</sub>*, that is,  $V_{t_{i+1}}^j$  for *j* = 1, 2, 3 . . . , *M*, we generate random samples for  $\eta_{t_i}^{V,j}$  in Equation (5). Since  $\text{Corr}(\epsilon_{t_i}^S, \eta_{t_i}^V) = \rho$ , we draw samples of  $\eta_{t_i}^{V,j}$  according to

$$\eta_{t_i}^{V,j} = \rho \epsilon_{t_i}^{S,j} + \sqrt{1 - \rho^2} \epsilon_{t_i}^{V,j},$$

where  $\epsilon_{t_i}^{V,j} \sim \text{ND}(0, 1)$  (following the standard normal distribution), for *j* = 1, 2, 3 . . . , *M*. Equipped with  $\eta_{t_i}^{V,j}$ , we derive a set of simulated values of *V<sub>t<sub>i+1</sub></sub>* as

$$V_{t_{i+1}}^j - V_{t_i}^j = \kappa^P \left( \theta^P - V_{t_i}^j \right) \Delta t + \left[ \sigma_1 \left( V_{t_i}^j \right)^{0.5} D_1 \left( V_{t_i}^j \right) + \sigma_2 \left( V_{t_i}^j \right)^\gamma D_2 \left( V_{t_i}^j \right) \right] \sqrt{\Delta t} \eta_{t_i}^{V,j}$$

for the DCEV model.<sup>7</sup>

3.3 For the actual  $\ln S_{t_{i+2}}$ , the simulated particles  $V_{t_{i+1}}^j$ , and the estimated parameters in Step 1, we then calculate the likelihood value from the normal density for all *j*:

7 For the CEV and NLD models,  $V_{t_{i+1}}^j$  is simulated based on

$$V_{t_{i+1}}^j - V_{t_i}^j = \kappa^P \left( \theta^P - V_{t_i}^j \right) \Delta t + \sigma_2 \left( V_{t_i}^j \right)^\gamma \sqrt{\Delta t} \eta_{t_i}^{V,j}$$

and

$$W_{t_{i+2}}^j = \phi_1 (\ln S_{t_{i+2}}, \ln S_{t_{i+1}} + (\mu - q - 0.5V_{t_{i+1}}^j) \Delta t, V_{t_{i+1}}^j \Delta t).$$

3.4 The empirical cumulative distribution function of  $V_{t_{i+1}}^j$  is constructed by using  $W_{t_{i+2}}^j$  to calculate the normalized weights for  $V_{t_{i+1}}^j$ . We resample  $\tilde{V}_{t_{i+1}}^j$  based on the continuous approximation algorithm proposed in [Malik and Pitt \(2011\)](#), which results in a smoothed empirical cumulative distribution function for  $V_{t_{i+1}}^j$ . This resampling process effectively reduces the discretization error caused by examining a limited number of particles. The advantage of this approach is its speed and extensibility in implementation for a variety of applications. For details, see Appendices A1A3 of [Malik and Pitt \(2011\)](#). The filtered variance of model  $k$  at time  $t_{i+1}$ ,  $\hat{V}_{t_{i+1}}^k$ , is simply the average of the resampled  $\tilde{V}_{t_{i+1}}^j$ :

$$\hat{V}_{t_{i+1}}^k = \frac{1}{M} \sum_{j=1}^M \tilde{V}_{t_{i+1}}^j.$$

We treat  $\hat{V}_{t_{i+1}}^k$  as the forecasting variance at time  $t_{i+1}$  of the model  $k$ . Repeating Steps 3.13.4 at time  $t_{i+2}, t_{i+3}, \dots$ , and  $t_{i+D}$ , we obtain  $\hat{V}_{t_{i+2}}^k, \hat{V}_{t_{i+3}}^k, \dots$ , and  $\hat{V}_{t_{i+D}}^k$ .

Step 4. Following [Mijatovic and Schneider \(2014\)](#), we calculate the  $D$ -day-ahead forecasting average variance (FV) generated from the model  $k$  on date  $t_i$  as

$$FV_{t_{i+D}}^k = \frac{1}{D} \sum_{l=1}^D \hat{V}_{t_{i+l}}^k.$$

Step 5. By rolling the window forward by  $D$  days, the re-estimated parameters on a new date  $t_i$  are utilized to forecast variance over the period covering  $t_{i+1}, t_{i+2}, \dots, t_{i+D}$ . Whenever we add  $D$  more observations into the sample, the most aged  $D$  observations in the sample are discarded such that the number of samples for estimation remains 1,000. Steps 1–5 are repeated until we reach the end of the sample.

Note that it is critical to account for the information on the realized innovations of spot prices in the out-of-sample test by applying the particle filter approach to examining SV models (see Step 3 above), as the volatility is nonobservable and merely a kind of statistic information embedded in spot prices. We argue that one should not simply simulate the  $\eta_t^V$ s from the standard normal distribution based on the stochastic variance process individually and next calculate the expected variance for  $D$ -day-ahead horizons, as this approach does not yield trustworthy forecasts of the variance for the estimated parameters, because the correlation between the innovations of the spot price and variance is ignored. This indicates another important reason for our estimation of the examined SV models with both time series of  $S_t$  and  $V_t$ . Since we employ the information of both  $S_t$  and  $V_t$  in the in-sample and out-of-sample tests, the methodology in this paper is internally consistent and is employed in [Eraker \(2004\)](#) and [Kaeck and Alexander \(2012\)](#) also.

For each forecasting variance, we follow [Mijatovic and Schneider \(2014\)](#) in calculating the average of annualized 5-min RV (AV) on dates  $t_{i+1}, t_{i+2}, \dots, t_{i+D}$  as the corresponding benchmark, that is,

$$V_{t_{i+1}}^j - V_{t_i}^j = \left[ \alpha_0 + \alpha_1 V_{t_i}^j + \alpha_2 (V_{t_i}^j)^2 + \alpha_3 (V_{t_i}^j)^{-1} \right] \Delta t + \sigma (V_{t_i}^j)^\gamma \sqrt{\Delta t} \eta_{t_i}^{V,j},$$

respectively.

$$AV_{t_{i+D}} = \frac{1}{D} \sum_{l=1}^D 252 \cdot RV_{t_{i+l}}.$$

After obtaining the series of FVs and AVs under the rolling window scheme, we compute the MSEs to measure the forecasting ability of each model:

$$MSE_{out}^k = \frac{\sum_{i=1}^n (FV_{t_{i+D}}^k - AV_{t_{i+D}})^2}{n},$$

where  $k = \text{DCEV, CEV, and NLD}$ , and  $n$  is the number of rolling times, computed as the largest integral smaller than  $(N - 1000)/D$ . We also evaluate the statistical significance of  $MSE_{out}$  differences between DCEV model and the competing models with the following pairwise  $t$ -statistic:

$$t - \text{statistic} = \frac{MSE_{out}^{DCEV} - MSE_{out}^k}{\bar{\sigma}_{DCEV,k}},$$

where  $k = \text{CEV and NLD}$ , and  $\bar{\sigma}_{DCEV,k}$  is the standard deviation of the difference of the squared error on each forecasting date. We adjust the standard deviation calculation for serial dependence based on [Newey and West \(1987\)](#). A negative (positive)  $t$  statistic means that the MSE of the benchmarked DCEV model is smaller (larger) than that of the competing models.

For out-of-sample option pricing experiments, the same rolling window estimation scheme described above is adopted, and we focus on pricing S&P 500 index call and put options with 30 days to maturity (approximately 21 trading days and thus the time maturity being 21/252 here), since the proposed estimation method in this paper utilizes the information of VIX, which is designed to reflect the volatility of the S&P 500 index in the period of future 30 days. We employ the discrete-time counterpart of [Equation \(2\)](#) (with a time step of  $\frac{1}{50}$  to mitigate discretization error) and the Monte Carlo simulation with 10,000 paths to compute the option prices for the DCEV, CEV, and SQR models. However, to conduct this simulation approach, we require not only the estimated parameter values in [Equation \(2\)](#) but also the initial value of the variance on an examined date  $t_i$ . The former can be obtained according to the estimation results of the rolling window scheme up to  $t_i$ , but the latter necessitates further estimation. We argue that using  $V_{t_i}$  inferred from  $VIX_{t_i}$  to evaluate options on an examined date  $t_i$  may incur foresight bias, because  $VIX_{t_i}$  is actually determined based on the option prices on date  $t_i$ . To mitigate this problem, we derive an estimation  $\widehat{VIX}_{t_i}^2$  based on the following regression for the whole-sample period:

$$VIX_{t_i}^2 = \beta_0 + \sum_{j=1}^p \beta_j VIX_{t_{i-j}}^2 + v_{t_i},$$

where  $v_{t_i} \sim N(0, \sigma_v)$ . The adjusted  $R^2$  values of the regression for  $p = 1, 2, 3,$  and  $4$  are 0.940974, 0.941715, 0.942716, and 0.942715, respectively, so we choose  $p = 3$  (with a higher adjusted  $R^2$  than that of  $p = 4$ ) to avoid overidentification.

In summary, on an examined date  $t_i$ , we obtain  $\widehat{VIX}_{t_i}^2 = \hat{\beta}_0 + \sum_{j=1}^3 \hat{\beta}_j VIX_{t_{i-j}}^2$  and then transform  $\widehat{VIX}_{t_i}^2$  to  $\hat{V}_{t_i}$  using [Equation \(4\)](#) for the DCEV, CEV, and SQR models given the up-to- $t_i$  parameters estimated by the rolling window scheme. Next, we simulate the system

of stochastic difference equations in Equation (2) given  $S_{t_i}$  and  $\hat{V}_{t_i}$  (to approximate  $V_{t_i}$ ), and obtain the theoretical call and put values with different strike prices through computing the present values of their expected payoffs at maturity under the risk-neutral measure. Note that the risk-free interest rate  $r$  (used in the drift term of the spot price and for discounting the expected option payoff) is fixed as the one-month risk-free interest rate observed at  $t_i$ . Finally, we follow Broadie, Chernov, and Johannes (2007) and Kaeck and Alexander (2012) to measure the out-of-sample performance of the DCEV, CEV, and SQR models in terms of the root of the mean of the squared pricing errors (RMSEs) as follows:

$$\text{RMSE}_{\text{out}}^k = \sqrt{\frac{\sum_{t_i} \sum_{K_{ij}} \left( \text{OV}_{t_i, K_{ij}}^k - \text{MP}_{t_i, K_{ij}} \right)^2}{n_o}},$$

where  $k = \text{DCEV}, \text{CEV}, \text{and SQR}$ ,  $\text{OV}_{t_i, K_{ij}}^k$  and  $\text{MP}_{t_i, K_{ij}}$  denote, respectively, the theoretical option value based on the model  $k$  and its market price corresponding to different strike prices  $K_{ij}$  on an examined date  $t_i$ , and  $n_o$  is the number of total examined option contracts.

## 2 Empirical Results

The empirical data set for the in-sample test consists of daily prices of the S&P 500 and VIX indices from January 2, 1996 to December 29, 2017. Both time series are collected from Bloomberg, and the number of total data pairs is  $N = 5442$ . As a robustness check, we also split the whole sample of 1996–2017 into four sub-sample periods: the periods from 1996 to 2000, from 2001 to August of 2007, from September of 2007 to 2009 (the crisis period covering the subprime crisis and the subsequent financial tsunami), and from 2010 to 2017 (the after-crisis period). The first two sub-sample periods are in line with those examined in Duan and Yeh (2010) such that one can conduct a close comparison with their empirical results in these two subperiods.

For out-of-sample tests, we conduct variance forecasting (option pricing) experiments based on the estimated parameters under the physical (risk-neutral) measure, since one of the advantages of our estimation method for the DCEV model is that both the physical and risk-neutral parameter values can be obtained simultaneously through the estimation process. The daily data of the 5-min RVs (S&P 500 index options) are downloaded from the website of the Oxford-Man Institute (the database of OptionMetrics). Because the data of RVs are available since January 4, 2000 and the last date of the examined period of the in-sample test is December 29, 2017, for consistency, we constrain the examined period of the out-of-sample tests for both variance forecasting and option pricing to lie between these two dates.

For pricing options, the average of the bid and ask quotes is regarded as the market price for each option contract, the risk-free interest rate on each examined date is approximated by the continuously compounding Treasury zero rates with 30 calendar days to maturity provided by OptionMetrics, and the dividend yield  $q$  of the S&P 500 index is calculated based on the monthly data provided on Robert Shiller's website. Finally, the option contracts are screened according to the following criteria: (1) Since the VIX levels play critical roles in the proposed model and are highly related with the option-implied volatilities for the following 30 days, we focus on pricing European call and put options with 30 calendar days to maturity; (2) options with market prices below 3/8 dollars are filtered out according

to the common setting in the literature on S&P 500 index options; (3) option contracts with moneyness out of  $[0.9, 1.1]$  are excluded. We define moneyness as the ratio between the strike and spot price,  $K/S_0$ ; and (4) option contracts are eliminated if the Black-Scholes implied volatilities corresponding to their market prices do not exist. The above screening process results in a total of 50,711 contracts included for the out-of-sample option pricing test.

Table 3 provides the descriptive statistics of the S&P 500 index returns, the VIX index, and the annualized RV in the examined periods. As some RV data are not available for the sample period, the statistic quantities associated with the RV are reported only for the second to fourth subperiods. As observed in Table 3, the S&P 500 index returns exhibit negative skewness and heavy tails in the whole-sample period. The four subperiods all possess similar characteristics except for the positive skewness in the second subperiod. During the subprime crisis, starting at mid-2007, the volatility increased and the index price decreased dramatically; these volatile economic conditions continued until the end of 2009. One thus observes a negative average index return and a significantly higher average and standard deviation for the VIX index and RV in the third subperiod. The maximum and minimum ranges of the VIX index and RV are also widest in the third subperiod. For the VIX index and RV, they are positively skewed with heavy tails in all examined periods, particularly in the last two subperiods. In addition, we plot the time series of the S&P 500 index, the VIX index, and the annualized standard deviation of the S&P 500 index returns calculated for the subsequent 21 trading days (one-month calendar days). Figure 1 shows that the S&P 500 index suffers a dramatic downturn and the VIX and standard deviation of the S&P 500 index returns skyrocket in the subprime crisis and the following financial tsunami. Moreover, the VIX index is systematically higher than the standard deviation of the S&P 500 index returns over the whole examined period, which suggests that the volatility risk has mostly been priced by the market according to Duan and Yeh (2010).

In the following in-sample and out-of-sample variance forecasting analyses, we investigate the performance of the DCEV, CEV, and NLD models in the whole-sample period and four subperiods. By contrasting the performance of the DCEV model with that of the CEV model, one can discern the advantage of introducing the damping function into the conventional CEV model. Moreover, we intentionally examine the NLD model, modified by imposing the  $V_t$ -VIX $_t^2$  linear transformation such that the differences in the performance of the DCEV and NLD models truly reflect the model superiority of the LD plus the DCEV diffusion over that of the NLD plus the CEV diffusion. As for the out-of-sample option pricing analyses, the SQR model replaces the NLD model as a competing model because the latter lacks the estimation for risk-neutral parameters. In addition, the potential advantage and possible usefulness of the DCEV model in option pricing is further demonstrated if the DCEV model outperforms the SQR model, which in practice is commonly used for option pricing.

## 2.1 In-Sample Analysis

The maximum-likelihood estimation results for the DCEV, CEV, and NLD models in the whole-sample period and four subperiods are reported in Tables 4–8, respectively. It is well known that a model with more parameters is likely to yield a higher LL value but can cause an illusion of better performance due to overfitting. In order to measure the in-

**Table 3** Descriptive statistics in different periods

Period	Whole sample	Subsamples			
		1996–2017	1996–2000	2001–2007/08	2007/09–2009
S&P 500 daily return					
Mean	0.0003	0.0006	0.0001	−0.0005	0.0004
Standard deviation	0.0120	0.0115	0.0108	0.0210	0.0094
Skewness	−0.2360	−0.2354	0.0446	−0.1277	−0.4639
Kurtosis	10.9598	5.7980	5.8185	7.7449	7.7994
Maximum	0.1096	0.0499	0.0557	0.1096	0.0463
Minimum	−0.0947	−0.0711	−0.0505	−0.0947	−0.0690
VIX					
Mean	20.2988	22.3963	18.9136	30.7079	17.0884
Standard deviation	8.3278	5.2446	7.2055	12.8670	5.9633
Skewness	1.9831	1.0809	1.0293	1.5672	1.6936
Kurtosis	9.8636	5.1178	3.4211	4.9051	6.4495
Maximum	80.8600	45.7400	45.0800	80.8600	48.0000
Minimum	9.1400	12.0000	8.8900	16.1200	9.1400
$\sqrt{RV}$ (%)					
Mean			12.9338	23.5443	11.0045
Standard deviation			6.8584	15.7103	7.3045
Skewness			1.9780	2.3934	3.0400
Kurtosis			8.8616	11.3023	20.8044
Maximum			57.9000	139.7294	96.9471
Minimum			3.6477	5.4669	1.7534

*Notes:* Both series of daily S&P 500 and VIX indices are collected from Bloomberg, covering the period from January 1996 to December 2017. The time series of daily 5-min RV (realized variance) is downloaded from the website of the Oxford-Man Institute. Since the earliest available date for the 5-min RV is January 4, 2000, the statistics analysis of  $\sqrt{RV}$  is conducted on neither the whole-sample period nor the subperiod from 1996 to 2000.

sample fitting performance fairly, we report not only the LL value but also the AIC value, which discourages overfitting with the addition of a penalty function that increases with the number of parameters. In addition, [Hong and Li's \(2005\)](#)  $Q$ -statistic is calculated to compare the appropriateness of different model specifications. [Hong and Li \(2005\)](#) argue that as there may exist other features not explored in the specification of examined models, there is a long way to go to obtain a significant  $Q$ -statistic even for the most sophisticated model examined in their paper. Consequently, they merely compare the relative levels of  $Q$ -statistics and identify a more appropriate model specification according to a smaller  $Q$ -statistic value. We also follow [Hong and Li \(2005\)](#) to evaluate the relative performance of the examined SV models in terms of the magnitude of the  $Q$ -statistic.



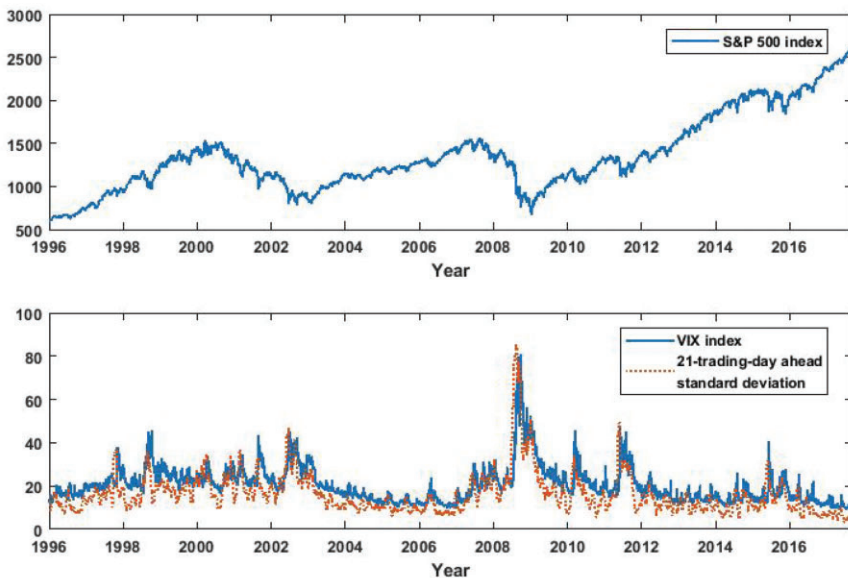


**Figure 1** S&P 500 index, VIX index, and 21-trading-day-ahead standard deviations (annualized and multiplied by 100) of S&P 500 index returns.

In Table 4, the DCEV model dominates the other two competing models in terms of its higher LL value, lower AIC value, and smaller  $Q$ -statistic in the whole-sample period. It is not surprising that the DCEV model outperforms the CEV model, but it is encouraging that the DCEV model performs better than the NLD model. Since the NLD model examined here possesses several desirable features to enhance its performance, the fact that the DCEV model still outperforms the NLD model under such unfavorable settings firmly establishes the contribution made by the proposed DCEV model. Recall that for the original NLD model, it is not feasible to use  $VIX_t$  information to analytically infer unobservable  $V_t$ . In fact, without the  $V_t$ - $VIX_t^2$  transformation, the performance of the original NLD model is far worse than the NLD model examined here. To account for this shortcoming of the NLD model, this paper is the first to utilize the data-implied linear  $V_t$ - $VIX_t^2$  transformation in Equation (8) to approximate the latent  $V_t$  according to the prevailing  $VIX_t$  index. In Table 4, the estimated values for both  $a$  and  $b$  are significant, which demonstrates the satisfactory performance of this linear approximation and also the sufficient marginal benefit of adding these two parameters to the NLD model. Recall that the main advantage of the NLD model over the DCEV model is its more general drift term. Despite the many advantages of the NLD model, its performance is still inferior to that of the DCEV model in terms of all three measurements. Other interesting findings in Tables 4–8 are discussed as follows.

First, the superiority of the DCEV model over the CEV model verifies that introducing the damping function into the CEV diffusion term more properly captures volatility dynamics. In addition, the lower AIC values of the DCEV model prove that the improvements of the DCEV model are due to the novel specification of the damping function rather than the

**Table 4** Maximum-likelihood estimation results for whole-sample period from January 2, 1996 to December 29, 2017

Parameter	DCEV	CEV	Parameter	NLD
$\kappa^p$	1.8116** (0.5085)	0.4024 (0.4380)	$\alpha_0$	0.0264 (0.0395)
$\theta^p$	0.0413** (0.0096)	0.1127 (0.1177)	$\alpha_1$	0.3865 (1.6015)
$\sigma_1$	0.2126** (0.0096)		$\alpha_2$	-18.1019 (12.2112)
$\sigma_2$	4.4312** (0.2322)	1.9923** (0.0362)	$\alpha_3$	0.0002 (0.0002)
$\rho$	-0.7850** (0.0045)	-0.7833** (0.0045)	$\sigma$	2.1026** (0.0471)
$\gamma$	1.3856** (0.0236)	0.9448** (0.0065)	$\rho$	-0.7841** (0.0045)
$\delta_V$	-9.0001** (0.5185)	-8.9076** (0.5045)	$\gamma$	0.9703** (0.0080)
			$a$	-0.0009** (0.0002)
			$b$	0.6624** (0.0126)
LL	41304	41247		41254
AIC	-82595	-82483		-82490
Q-statistic	17.2440	17.2980		17.6208

Notes: This table reports the estimated parameters, standard errors (in parentheses), LL values, AIC values, and Hong and Li's (2005) Q-statistics for different models using maximum-likelihood estimation. The standard errors are calculated by estimating the inverse of the Fisher information matrix using an outer product of gradients method at the optimal parameter values. The asterisks indicate parameter significance at the 5% (\*\*) and 10% (\*) significance levels.

use of additional parameters. Moreover, the estimated exponent term ( $\gamma$ ) of the DCEV model is always significantly higher than 1.2 (in the crisis period, even higher than 2), but that of the CEV model is close to or lower than 1. We conjecture that the  $\gamma$  in the CEV model may be self-constrained to be artificially low to avoid unreasonably explosive behavior when  $V_t$  is high.<sup>8</sup> The relatively low value of  $\gamma$  in the CEV model may harm its overall fitting performance regardless of whether  $V_t$  is high or low. Since the damping function effectively controls this explosive behavior when  $V_t$  is high, the constraint for  $\gamma$  in the DCEV model is removed and thus  $\gamma$  in the DCEV model reflects its actual nature. In summary, despite the minor difference in specifications between the DCEV and CEV models, the effect of introducing the damping function is comprehensive rather than merely imposing a cut when  $V_t$  is high.

8 In Tables 4–8, the estimated values of  $\gamma$  in the NLD model always lie between those of the DCEV and CEV models. We conjecture that the self-constrained effect for  $\gamma$  in the NLD model may not be so serious (compared with the CEV model) due to the nonlinear drift term which can reinforce the mean-reverting behavior.

**Table 5** Maximum-likelihood estimation results for sub-sample period from January 2, 1996 to December 29, 2000

Parameter	DCEV	CEV	Parameter	NLD
$\kappa^p$	2.1381* (1.2099)	1.4941 (1.1661)	$\alpha_0$	-0.1004 (0.3274)
$\theta^p$	0.0506** (0.0194)	0.0605* (0.0345)	$\alpha_1$	3.9107 (11.5862)
$\sigma_1$	0.2418** (0.0281)		$\alpha_2$	-77.5606 (118.2668)
$\sigma_2$	9.4844* (5.0589)	1.6555** (0.1479)	$\alpha_3$	0.0024 (0.0027)
$\rho$	-0.7386** (0.0093)	-0.7369** (0.0087)	$\sigma$	2.5014** (0.4250)
$\gamma$	1.7705** (0.2120)	0.9342** (0.0314)	$\rho$	-0.7431** (0.0090)
$\delta_V$	-10.2793** (0.9703)	-10.1655** (0.9603)	$\gamma$	1.1128** (0.0627)
			$a$	0.0024 (0.0015)
			$b$	0.5550** (0.0333)
LL	9047	9039		9050
AIC	-18080	-18066		-18082
Q-statistic	3.0973	3.1206		3.6555

Notes: This table reports the estimated parameters, standard errors (in parentheses), LL values, AIC values, and Hong and Li's (2005) Q-statistics for different models using maximum-likelihood estimation. The standard errors are calculated by estimating the inverse of the Fisher information matrix using an outer product of gradients method at the optimal parameter values. The asterisks indicate parameter significance at the 5% (\*\*) and 10% (\*) significance levels.

Second, even though there are fewer parameters in the DCEV model than in the NLD model, the DCEV model outperforms the NLD model in all examined periods except the sub-sample period from January 1, 1996 to December 29, 2000 reported in Table 5, where the LL (AIC) values of NLD model are larger (smaller) than those of the DCEV model. However, the smaller Q-statistic of the DCEV model in Table 5 indicates that it is still closer to the true volatility dynamic than the NLD model. As mentioned in the analyses for the whole-sample-period results in Table 4, the NLD model examined here enjoys extra benefits, so it is reasonable that the NLD model sometimes outperforms the DCEV model given different datasets. Nevertheless, even under this not-quite-fair comparison, the superior performance of the DCEV model over the NLD model is readily apparent in Tables 4–8, which confirms our assertion that the DCEV model is more appropriate than the NLD model commonly found in the literature for describing the SV process.

Last, our two-step estimation procedure generates consistent estimation results for the diffusion-related estimators ( $\sigma_2$ ,  $\gamma$ , and  $\rho$ ) with those in Duan and Yeh (2010) in the first two sub-sample periods, as reported in Tables 5 and 6. Take the period of January 2001 to August 2007 for example. Table 6 [Table 2 in Duan and Yeh (2010)] shows estimated

**Table 6** Maximum-likelihood estimation results for sub-sample period from January 2, 2001 to August 31, 2007

Parameter	DCEV	CEV	Parameter	NLD
$\kappa^P$	1.6149* (0.9275)	1.1017 (0.8076)	$\alpha_0$	-0.1019 (0.1127)
$\theta^P$	0.0326** (0.0134)	0.0390* (0.0235)	$\alpha_1$	4.8410 (5.1924)
$\sigma_1$	0.1622** (0.0201)		$\alpha_2$	-70.3960 (58.1803)
$\sigma_2$	2.9284** (0.4646)	1.3643** (0.0577)	$\alpha_3$	0.0009 (0.0006)
$\rho$	-0.7755** (0.0103)	-0.7753** (0.0103)	$\sigma$	1.4963** (0.0884)
$\gamma$	1.3013** (0.0695)	0.8854** (0.0148)	$\rho$	-0.7763** (0.0102)
$\delta_V$	-8.9115** (0.9497)	-8.8866** (0.9399)	$\gamma$	0.9293** (0.0215)
			$a$	-0.0003 (0.0005)
			$b$	0.6607** (0.0301)
LL	12938	12931		12936
AIC	-25861	-25849		-25854
Q-statistic	7.4642	7.4812		7.5353

Notes: This table reports the estimated parameters, standard errors (in parentheses), LL values, AIC values, and Hong and Li's (2005) Q-statistics for different models using maximum-likelihood estimation. The standard errors are calculated by estimating the inverse of the Fisher information matrix using an outer product of gradients method at the optimal parameter values. The asterisks indicate parameter significance at the 5% (\*\*) and 10% (\*) significance levels.

values for  $\sigma_2$ ,  $\gamma$ , and  $\rho$  being 1.3643, 0.8854, and -0.7753 (1.3572, 0.8942, and -0.7753), respectively. As for the drift-related parameters ( $\kappa^P$  and  $\theta^P$ ) and the market prices of volatility risk ( $\delta_V$ ), our estimation results differ slightly from those in Duan and Yeh (2010). Note that all of these parameters could affect the drift terms of the spot price and volatility processes during the transformation between the physical and risk-neutral measures. Whereas Duan and Yeh (2010) estimate all the parameters in the drift term of the spot price, recall that our two-step estimation procedure fixes the drift term of  $\mu - q$  in the spot price dynamic as the annualized arithmetic average of the daily returns. Furthermore, note that the market prices of volatility risk ( $\delta_V$ ) are significantly negative across the DCEV and CEV models in all examined periods except for the estimators of the CEV model in the crisis period, where  $\delta_V$  is negative but not significant. These observations are in line with the results reported in Duan and Yeh (2010) and imply that the volatility risk premiums are properly priced by the DCEV and CEV models in most examined periods.

Overall, the in-sample analyses attest the superiority of the proposed DCEV model over the conventional CEV and NLD models, even though the NLD model is additionally

**Table 7** Maximum-likelihood estimation results for sub-sample period from September 4, 2007 to December 31, 2009[TQ38]

Parameter	DCEV	CEV	Parameter	NLD
$\kappa^p$	2.3115 (1.5917)	0.1361 (1.4305)	$\alpha_0$	-0.7767 (0.5721)
$\theta^p$	0.1002** (0.0509)	0.9979 (10.1757)	$\alpha_1$	10.2208 (8.3114)
$\sigma_1$	0.4404** (0.0437)		$\alpha_2$	-26.5274 (24.4772)
$\sigma_2$	7.8067** (1.0977)	2.8598** (0.1214)	$\alpha_3$	0.0202 (0.0106)
$\rho$	-0.8438** (0.0101)	-0.8442** (0.0109)	$\sigma$	2.9453** (0.1577)
$\gamma$	1.8819** (0.1058)	1.0385** (0.0277)	$\rho$	-0.8446** (0.0112)
$\delta_V$	-3.6181** (1.4095)	-2.1782 (1.5812)	$\gamma$	1.0693** (0.0347)
			$a$	-0.0028 (0.0029)
			$b$	0.8803** (0.0589)
LL	3663	3649		3652
AIC	-7312	-7293		-7286
Q-statistic	5.1348	5.1793		5.1405

Notes: This table reports the estimated parameters, standard errors (in parentheses), LL values, AIC values, and Hong and Li's (2005) Q-statistics for different models using maximum-likelihood estimation. The standard errors are calculated by estimating the inverse of the Fisher information matrix using an outer product of gradients method at the optimal parameter values. The asterisks indicate parameter significance at the 5% (\*\*) and 10% (\*) significance levels.

equipped with a data-implied  $V_t$ -VIX $_t^2$  linear transformation. The outstanding fitting performance of the DCEV model is significant and robust in all examined periods. We suggest that instead of using the NLD model or the pure CEV model, the DCEV model may be a more suitable candidate to characterize the volatility dynamics.

### 2.2 Out-of-Sample Analysis

This subsection presents the results of two out-of-sample tests to prove the superior practicability of the DCEV model. Since we require 1,000 observations to obtain the first set of parameter estimations in the rolling window scheme, the starting month for the out-of-sample tests is January 2000 rather than January 1996.

For variance forecasting, Table 9 reports MSE $_{out}$  results of the three examined SV models and pairwise  $t$ -statistics of the DCEV model versus the other two competing models in the whole-sample period. For robustness check, the MSE $_{out}$  and pairwise  $t$ -statistics in individual subperiods are reported in Table 10. Bold figures indicate the value of the smallest MSE $_{out}$  among the competing models. Since the DCEV model serves as the benchmark, the pairwise  $t$ -statistics versus the CEV and NLD models are shown in the parentheses next to

**Table 8** Maximum-likelihood estimation results for sub-sample period from January 4, 2010 to December 29, 2017

Parameter	DCEV	CEV	Parameter	NLD
$\kappa^p$	3.3999** (1.0419)	0.9809 (0.8686)	$\alpha_0$	-0.0329 (0.0791)
$\theta^p$	0.0237** (0.0055)	0.0483 (0.0390)	$\alpha_1$	4.0746 (5.0684)
$\sigma_1$	0.2349** (0.0159)		$\alpha_2$	-90.7512 (72.7280)
$\sigma_2$	12.3413** (1.2607)	3.0326** (0.1179)	$\alpha_3$	0.0004 (0.0003)
$\rho$	-0.8202** (0.0071)	-0.8177** (0.0071)	$\sigma$	3.2237** (0.1594)
$\gamma$	1.5836** (0.0373)	1.0076** (0.0131)	$\rho$	-0.8189** (0.0073)
$\delta_V$	-11.5431** (0.9541)	-10.9640** (0.9083)	$\gamma$	1.0319** (0.0161)
			$a$	-0.0012** (0.0003)
			$b$	0.6194** (0.0208)
LL	15938	15908		15910
AIC	-31861	-31803		-31802
Q-statistic	9.8973	10.5673		10.8170

Notes: This table reports the estimated parameters, standard errors (in parentheses), LL values, AIC values, and Hong and Li's (2005) Q-statistics for different models using maximum-likelihood estimation. The standard errors are calculated by estimating the inverse of the Fisher information matrix using an outer product of gradients method at the optimal parameter values. The asterisks indicate parameter significance at the 5% (\*\*) and 10% (\*) significance levels.

their MSEs. A negative (positive)  $t$ -statistic means that the MSE of the benchmarked DCEV model is smaller (larger) than that of the competing model. In Tables 9 and 10, several phenomena are worth discussing.

First, it can be observed in Table 9 that the DCEV model outperforms all other models in forecasting future 5-, 10-, and 15-day-ahead average RV in terms of its smallest MSEs. On average, the MSE of the DCEV model is smaller than that of the CEV and NLD models by 16.1% and 14.2%, respectively, in the whole-sample period. In addition, all pairwise  $t$ -statistics are significantly negative, which indicates that the forecasting errors of the DCEV model are significantly smaller than those of the competing models in the whole-sample period. Note that due to the similarity between the DCEV and CEV models, the standard deviation of the differences in MSEs between the DCEV and CEV models is generally smaller than that between the DCEV and NLD models. As a result, the pairwise  $t$ -statistics between the MSEs of the DCEV and CEV models are inclined to be more significant. In fact, they are all 5% level significant in Table 9; in contrast, the pairwise  $t$ -statistics between the MSEs of the DCEV and NLD models are all 10% level significant. Moreover, even though the DCEV outperforms the CEV model by a smaller amount (4.4452 versus

**Table 9** Out-of-sample MSEs of various SV models for whole-sample period from January 2000 to December 2017

<i>D</i> -day-ahead	5	10	15
DCEV	<b>7.9469</b>	<b>6.1765</b>	<b>4.4452</b>
CEV	9.3150 (−2.5246**)	7.5430 (−2.1658**)	5.2602 (−2.0716**)
NLD	8.7420 (−1.5045*)	7.1093 (−1.5230*)	5.5738 (−1.3119*)

*Notes:* This table reports the out-of-sample results of 5-, 10-, and 15-day-ahead variance forecasting under the rolling window scheme. The model performance is evaluated by the mean-squared error calculated from the out-of-sample fit ( $MSE_{out}$ ) multiplied by  $10^4$ . Bold entries represent the value of the smallest  $MSE_{out}$  among competing models. The pairwise  $t$ -statistics are shown in parentheses next to the MSEs of the CEV and NLD models. A negative (positive)  $t$ -statistic means that the MSE of the benchmarked DCEV model is smaller (larger) than that of the competing model. The asterisks indicate significance of the differences at the 5% (\*\*) and 10% (\*) significance levels.

5.2602) in MSEs than that for the NLD model (4.4452 versus 5.5738) in the 15-day-ahead case, it is still possible that the pairwise  $t$ -statistic between the MSEs of the DCEV and CEV models is more significant than that of the DCEV and NLD models.

Second, the superior forecasting performance of the DCEV model is again verified in 11 out of the 12 cases examined in Table 10. The only exception is the 15-day-ahead case in the subperiod January 2000–December 2000. Although the NLD performs best in this case in terms of its smallest MSE (2.0761), the pairwise  $t$ -statistic does not support the significance of this superiority. We attribute this exception to the insufficient sample size in this subperiods, which has a horizon of only one year, far shorter than the other three subperiods.

Third, it can be observed that the performance of the CEV model is close to that of the DCEV model in the first two subperiods but is far worse than that of the DCEV model or sometimes inferior to the NLD model in the last two subperiods. We attribute the relatively poor performance of the CEV model in September 2007–December 2009 and January 2010–December 2017 to the questionable estimations for its exponent term  $\gamma$  to avoid explosive behavior, since the high volatility in the financial crisis and subsequent period exacerbate this problem. Note that high volatility is more likely in the last two subperiods (compared with the first two subperiods), since the skewness (maximum value) of  $\sqrt{RV}$  is 1.8423, 1.9780, 2.3934, and 3.0400 (56.2451, 57.9000, 139.7294, and 96.9471) in the four subperiods, respectively.<sup>9</sup> In contrast, by combining the damping function into the CEV diffusion, the proposed DCEV model mitigates this disadvantage associated with the CEV model and still performs satisfactorily in the last two periods. This further explains why the DCEV model outperforms the CEV model insignificantly (significantly) in the first (last) two subperiods. This is because the degree of similarity between the DCEV and CEV models should be high for the low-volatility (first two) subperiods but diverge in the high-volatility (last two) subperiods.

9 These figures can be found in Table 3 except those for the first subperiod of January 2000–December 2000. In this subperiod, the mean, standard deviation, skewness, kurtosis, maximum value, and minimum value of  $\sqrt{RV}$  are 17.7169, 6.8743, 1.8423, 9.4668, 56.2451, and 7.1528, respectively.

**Table 10** Out-of-sample MSEs of various SV models for sub-sample periods

D-day-ahead	5	10	15
Forecasting period: January 2000–December 2000			
DCEV	<b>2.9610</b>	<b>1.5723</b>	2.1528
CEV	2.9645 (−0.2231)	1.5769 (−0.6455)	2.1708 (−0.8888)
NLD	3.4258 (−2.0664**)	1.8859 (−1.6980**)	<b>2.0761</b> (0.0375)
Forecasting period: January 2001–August 2007			
DCEV	<b>2.0164</b>	<b>1.8074</b>	<b>1.4939</b>
CEV	2.0197 (−0.1033)	1.8450 (−1.0214)	1.5050 (−0.8342)
NLD	2.1348 (−0.5402)	1.9658 (−0.6526)	1.6446 (−0.6553)
Forecasting period: September 2007–December 2009			
DCEV	<b>41.8339</b>	<b>33.2971</b>	<b>21.7575</b>
CEV	46.2449 (−1.5359*)	38.6686 (−1.3726*)	24.2039 (−1.3602*)
NLD	47.0093 (−1.5797*)	39.2344 (−1.4351*)	29.2376 (−1.1683)
Forecasting period: January 2010–December 2017			
DCEV	<b>3.5369</b>	<b>2.4090</b>	<b>2.0452</b>
CEV	5.3096 (−2.3613**)	3.8681 (−1.8020**)	3.1386 (−1.5556*)
NLD	3.6495 (−0.9445)	2.5923 (−1.3227*)	2.2508 (−1.2088)

*Notes:* This table reports the out-of-sample results of 5-, 10-, and 15-day-ahead variance forecasting under the rolling window scheme. The model performance is evaluated by the mean-squared error calculated from the out-of-sample fit ( $MSE_{out}$ ) multiplied by  $10^4$ . Bold entries represent the value of the smallest  $MSE_{out}$  among competing models. The pairwise  $t$ -statistics are shown in parentheses next to the MSEs of the CEV and NLD models. A negative (positive)  $t$ -statistic means that the MSE of the benchmarked DCEV model is smaller (larger) than that of the competing model. The asterisks indicate significance of the differences at the 5% (\*\*), and 10% (\*) significance levels.

Fourth, the NLD model usually performs the worst in the first three subperiods but yields competitive performance in the last subperiod. Note that in a time period where the volatility is highly positively skewed but the standard deviation of the volatility is at a normal level (see the descriptive statistics of  $\sqrt{RV}$  for the last subperiod in Table 3), the mean-reverting drift term plays a more important role than the not-so-volatile diffusion term for governing the dynamics of an SV process.<sup>10</sup> Furthermore, the NLD term in the NLD model is better able to capture the mean-reverting behavior than the conventional CEV model with a LD term. As a result, the NLD model outperforms the CEV model in the last subperiod. However, the superiority of the DCEV model over the NLD model still holds in the last subperiod, supporting our assertion that the DCEV model is more appropriate than the NLD model for describing the mean-reverting behavior of an SV process. Recall that the

10 In contrast, for the third subperiod (the financial crisis period), the volatility is not only highly positively skewed but its standard deviation is also relatively high. Consequently, the comparative effect of the mean-reverting drift term may be weakened due to a more volatile diffusion term.



NLD model examined in this paper enjoys benefits that make for an unfair comparison. Without introducing the data-implied  $VIX_t^2-V_t$  transformation in Equation (8), the NLD model performs even worse than the CEV model in the last subperiod.<sup>11</sup> This implies that the existence of the transformation between  $VIX_t$  and  $V_t$  is critical for estimating an SV model and also highlights the merits of the proposed DCEV model that not only maintains the LD term such that there exists an analytic  $V_t-VIX_t^2$  transformation but also exhibits a superior ability over the widely examined NLD model for describing the mean-reverting behavior of an SV process.

In addition to the experiments in Tables 9 and 10 under the physical measure, we next present the empirical results of out-of-sample option pricing of the examined SV models based on the estimations of risk-neutral parameters. Table 11 presents the option pricing  $RMSE_{out}$  results of the DCEV, CEV, and SQR models in the whole-sample and sub-sample periods, and Table 12 further separates the samples in different periods into three categories by option moneyness. In these two tables, bold entries represent the value of the smallest  $RMSE_{out}$  among competing models. A negative (positive) percentage number in the parentheses next to the RMSE means that the RMSE of the benchmarked DCEV model is smaller (larger) than that of the competing model by the indicated percentage number. Overall speaking, similar to the results for out-of-sample variance forecasting, the DCEV model dominates the competing models in option pricing in Tables 11 and 12.

Table 11 shows that the DCEV model uniformly improves the option pricing errors of the CEV model by roughly 3.3–4.4% in all subperiods except the last one, in which the RMSE of the DCEV model is still smaller than that of the CEV model but only by 2.2%. In contrast, the DCEV model dramatically reduces the option pricing errors of the SQR model by 11.4–26.7% in different subperiods. Since the SQR model is widely used for option pricing in practice, the superiority of the DCEV model over the SQR model in option pricing attests another important merit of the DCEV model. In addition, in slight contrast to the out-of-sample results of variance forecasting, in which the superiority of the DCEV model is more significant in the last two subperiods, the performance of the DCEV in option pricing is more pronounced in the second and third subperiods, especially versus the CEV model. Nevertheless, by combining the out-of-sample results of variance forecasting and option pricing, we have reason to believe the advantages of introducing the damping function in the CEV model may be amplified in a more volatile period, such as the financial crisis period, which is consistent with our original motivation for proposing the DCEV model.

In Table 12, the RMSEs of the DCEV model are smaller than those of the CEV and SQR models across all moneyness in all subperiods. In addition, the improvement of the DCEV model appears more pronounced for the moneyness in [0.97, 1.03] and larger than 1.03. Since variance is one of the many factors that influence option prices, it is not straightforward to explain all observed phenomena based only on the features of the DCEV model without controlling all other factors. However, the robust performance of the DCEV model in Table 12 is still encouraging to anyone who is interested in the DCEV model.

11 The related results are available from the authors upon request.

**Table 11** Out-of-sample RMSEs of S&P 500 index options

Model	Option contracts
Whole-sample period: January 2000–December 2017	
DCEV	<b>3.6148</b>
CEV	3.7015 (−2.34%)
SQR	4.8880 (−26.05%)
Sub-sample period: January 2000–December 2000	
DCEV	<b>3.8982</b>
CEV	4.0330 (−3.34%)
SQR	4.3979 (−11.36%)
Sub-sample period: January 2001–August 2007	
DCEV	<b>2.3562</b>
CEV	2.4657 (−4.44%)
SQR	2.7983 (−15.80%)
Sub-sample period: September 2007–December 2009	
DCEV	<b>3.2689</b>
CEV	3.3987 (−3.82%)
SQR	4.2188 (−22.52%)
Sub-sample period: January 2010–December 2017	
DCEV	<b>3.7343</b>
CEV	3.8175 (−2.18%)
SQR	5.0922 (−26.67%)

*Notes:* This table reports out-of-sample results on pricing S&P 500 index call and put option contracts with 30 calendar days to maturity. The model performance is evaluated by the root mean-squared errors ( $RMSE_{out}$ ) of all option contracts in an examined period. Bold entries represent the value of the smallest  $RMSE_{out}$  among competing models. A negative (positive) percentage number in parentheses next to the RMSE means that the RMSE of the benchmarked DCEV model is smaller (larger) than that of the competing model by the indicated percentage number.

### 3 Conclusion

We advocate a novel SV model with an LD and damped CEV diffusion. This structure captures similar or even more appropriate mean-reverting behavior than the commonly used NLD model proposed by [Ait-Sahalia \(1996\)](#) but lacks the complications of the NLD model. In addition, the proposed DCEV model also restrains the possibly explosive behavior of the traditional CEV model. Moreover, the specification of the DCEV model allows us to follow the estimation method proposed in [Duan and Yeh \(2010\)](#) to estimate the physical and risk-neutral parameters simultaneously after the latent volatility is inferred.

To comprehensively evaluate the performance of the proposed DCEV model, we compare not only in-sample fitting performance but also out-of-sample variance forecasting

**Table 12** Out-of-sample RMSEs of S&P 500 index options with different moneyness

Model	Moneyness		
	<0.97	0.97–1.03	>1.03
Whole-sample period: January 2000–December 2017			
DCEV	<b>2.2631</b>	<b>4.8925</b>	<b>2.9206</b>
CEV	2.2858 (–0.99%)	5.0049 (–2.24%)	3.0497 (–4.24%)
SQR	2.8462 (–20.49%)	6.5634 (–25.46%)	4.3734 (–33.22%)
Sub-sample period: January 2000–December 2000			
DCEV	<b>2.8753</b>	<b>4.5641</b>	<b>3.6955</b>
CEV	2.9265 (–1.75%)	4.7413 (–3.74%)	3.8222 (–3.31%)
SQR	3.0035 (–4.27%)	5.1628 (–11.60%)	4.2690 (–13.43%)
Sub-sample period: January 2001–August 2007			
DCEV	<b>1.3699</b>	<b>3.0331</b>	<b>2.1962</b>
CEV	1.3802 (–0.75%)	3.1635 (–4.12%)	2.3592 (–6.91%)
SQR	1.6797 (–18.45%)	3.5821 (–15.32%)	2.5995 (–15.51%)
Sub-sample period: September 2007–December 2009			
DCEV	<b>2.7530</b>	<b>3.7914</b>	<b>3.2067</b>
CEV	2.8174 (–2.29%)	3.9741 (–4.60%)	3.3357 (–3.87%)
SQR	3.1679 (–13.10%)	4.5968 (–17.52%)	4.6889 (–31.61%)
Sub-sample period: January 2010–December 2017			
DCEV	<b>2.2971</b>	<b>5.0974</b>	<b>2.9550</b>
CEV	2.3183 (–0.91%)	5.2064 (–2.09%)	3.0811 (–4.09%)
SQR	2.9105 (–21.08%)	6.8922 (–26.04%)	4.5220 (–34.65%)

*Notes:* This table reports out-of-sample results on pricing S&P 500 index call and put option contracts with 30 calendar days to maturity across different moneyness, which is defined as the ratio of the strike price to the underlying spot price. The model performance is evaluated by the root mean-squared errors (RMSE<sub>out</sub>) of the option contracts with specified moneyness in an examined period. Bold entries represent the value of the smallest RMSE<sub>out</sub> among competing models. A negative (positive) percentage number in parentheses next to the RMSE means that the RMSE of the benchmarked DCEV model is smaller (larger) than that of the competing model by the indicated percentage number.

with the physical parameters and option pricing with the risk-neutral parameters. The empirical results based on the time series of both the S&P 500 and VIX indices suggest that the DCEV model yields in-sample fitting performance that is superior to that of the CEV and NLD models and that the improvements yielded by the DCEV model arise from the advanced model specification rather than the inclusion of additional parameters.

In out-of-sample tests, we first apply the particle filter approach for variance forecasting, such that information on actual stock price innovations (the most original and

observable information) is taken into account when evaluating the forecasting power of the examined SV models. The DCEV model outperforms competing models statistically significantly in forecasting 5-, 10-, and 15-day-ahead average RVs for the whole sample and almost all subperiods. We next compare the model performance for option pricing based on the Monte Carlo simulation. The DCEV model consistently generates smaller pricing errors than the CEV and SQR models in evaluating S&P 500 index options across all moneyness in different examined periods. The impressive in-sample and out-of-sample empirical performance sheds light on the appropriateness of the proposed DCEV model to describe the volatility dynamics. Since this demonstrates that the DCEV model outperforms the NLD model (a classic representation of the nonaffine SV model), an interesting and fruitful future work would be to compare the proposed DCEV model with other innovative nonaffine SV models such as the stochastic log volatility model for various applications.

## Appendix A: Hong and Li's (2005) Q-Test for Examining SV Models

We first brief Hong and Li's (2005) Q-test method and then explain how to apply this method to test model specifications of the examined SV models.

Suppose that the stochastic process of the underlying variable  $\{Y_t\}$  follows

$$dY_t = \mu_0(Y_t, t)dt + \sigma_0(Y_t, t)dW_t,$$

where  $\mu_0(Y_t, t)$  and  $\sigma_0(Y_t, t)$  are the true drift and diffusion terms, and  $W_t$  is a standard Brownian motion. Let  $p_0(y, t|x, s)$  be the true transition density of  $Y_t$ ; that is, the conditional density of  $Y_t = y$  given  $Y_s = x$  and  $s < t$ . To examine a pair of  $\mu(Y_t, t, \hat{\Theta})$  and  $\sigma(Y_t, t, \hat{\Theta})$  (corresponding to a model specification with an estimated parameter set  $\hat{\Theta}$ ), a family of transition densities  $\{p(y, t|x, s, \hat{\Theta})\}$  is characterized. Hong and Li (2005) transform the sample  $\{Y_{i\Delta t}\}_{i=1}^N$  via the following dynamic probability integral transform:

$$Z_i(\hat{\Theta}) = \int_{-\infty}^{Y_{i\Delta t}} p(y, i\Delta t|Y_{(i-1)\Delta t}, (i-1)\Delta t, \hat{\Theta})dy, i = 1, \dots, N.$$

Hence, for some  $\theta_0$ , the hypotheses of interest  $\mathbb{H}_0$  that a model with the parameter set  $\theta_0$  is correctly specified can be written as

$$p(y, i\Delta t|Y_{(i-1)\Delta t}, (i-1)\Delta t, \theta_0) = p_0(y, i\Delta t|Y_{(i-1)\Delta t}, (i-1)\Delta t)$$

almost surely for all  $\Delta t > 0$ , and the series  $\{Z_i \equiv Z_i(\theta_0)\}_{i=1}^N$  follows i.i.d.  $U[0, 1]$  (standard uniform distribution).

The  $Z_i(\hat{\Theta})$  for  $i = 1, \dots, N$  are called the generalized residuals of model  $p(y, t|x, s, \hat{\Theta})$ . The main task is to test  $\mathbb{H}_0$  versus its alternative hypothesis by checking whether  $\{Z_i(\hat{\Theta})\}$  is i.i.d.  $U[0, 1]$  for some  $\hat{\Theta} = \theta_0$ . Hong and Li (2005) propose testing i.i.d.  $U[0, 1]$  by comparing a kernel estimator  $\hat{g}_j(z_1, z_2)$  for the joint density of  $\{\hat{Z}_i, \hat{Z}_{i-j}\}$  (the product of two  $U[0, 1]$  densities) with unity, where  $j$  is a prespecified lag order and  $\hat{Z}_i$  is the abbreviation of  $Z_i(\hat{\Theta})$ .

The kernel estimator of the joint density is, for any integer  $j > 0$ , as follows:

$$\hat{g}_j(z_1, z_2) = (N - j)^{-1} \sum_{i=j+1}^N K_b(z_1, \hat{Z}_i) K_b(z_2, \hat{Z}_{i-j}),$$

where  $K_b(z_1, z_2)$  is a boundary-modified kernel function defined as follows, for  $x \in [0, 1]$ ,

$$K_b(x, y) \equiv \begin{cases} b^{-1} k\left(\frac{x-y}{b}\right) / \int_{-\frac{x}{b}}^1 k(u) du & \text{if } x \in [0, b), \\ b^{-1} k\left(\frac{x-y}{b}\right) & \text{if } x \in [b, 1-b], \\ b^{-1} k\left(\frac{x-y}{b}\right) / \int_{-1}^{\frac{1-x}{b}} k(u) du & \text{if } x \in (1-b, 1], \end{cases}$$

where  $k(\cdot)$  is a prespecified symmetric probability density and  $b \equiv b(N)$  is a bandwidth such that  $b \rightarrow 0, Nb \rightarrow \infty$  as  $N \rightarrow \infty$ . [Hong and Li \(2005\)](#) choose a quartic kernel as follows.

$$k(u) = \frac{15}{16} (1 - u^2)^2 1(|u| \leq 1),$$

where  $1(\cdot)$  is the indicator function, and  $b = \hat{S}_Z N^{-1/6}$ , where  $\hat{S}_Z$  is the sample standard deviation of  $\{Z_i(\hat{\Theta})\}_{i=1}^N$ . Finally, the  $Q$ -statistic is defined as

$$Q(j) \equiv \left[ (N - j) b \hat{M}(j) - b A_b^0 \right] / V_0^{1/2},$$

where

$$\hat{M}(j) \equiv \int_0^1 \int_0^1 [\hat{g}_j(z_1, z_2) - 1]^2 dz_1 dz_2,$$

$$A_b^0 \equiv \left[ (b^{-1} - 2) \int_{-1}^1 k^2(u) du + 2 \int_0^1 \int_{-1}^b k_b^2(u) du db \right]^2 - 1,$$

$$V_0 \equiv 2 \left[ \int_{-1}^1 \left[ \int_{-1}^1 k(u+v) k(v) dv \right]^2 du \right]^2,$$

and  $k_b(\cdot) \equiv k(\cdot) / \int_{-1}^b k(v) dv$ . Under correct model specification, as  $N \rightarrow \infty$ ,

$$Q(j) \rightarrow \text{ND}(0, 1) \text{ in distribution.}$$

When  $Q(j)$  is computed, the larger the  $Q$ -statistic, the larger the departure from the true model. Moreover, [Hong and Li \(2005\)](#) mention that the first lag  $j = 1$  is often the most informative and important, so in our empirical analysis we report the  $Q$ -statistic with  $j$  equal to 1.

Since the actual variance process is nonobservable,<sup>12</sup> a possible alternative to apply the  $Q$ -test for model specification of the SV models examined in this paper is to utilize the actual time series  $\{Y_t = \ln(S_t)\}$  that can be observed from the market. Under this constraint,

12 Note that [Hong and Li's \(2005\)](#)  $Q$ -test utilizes discretely observed times series  $\{Y_t\}$  for testing the model specification. If one employs the inferred variance  $V_t$  to be  $Y_t$  when conducting [Hong and Li's \(2005\)](#)  $Q$ -test, since the inferred variance  $V_t$  is merely an approximation for the actual

our idea to apply the  $Q$ -test to the examined three SV models is as follows: as long as an SV model with an parameter set of  $\hat{\Theta}$  (estimated based on the proposed method in this paper) infers more appropriate variances (closer to the actual ones if they were observable), the corresponding  $\mu(Y_t, t, \hat{\Theta})$  and  $\sigma(Y_t, t, \hat{\Theta})$  should be closer to the true  $\mu_0(Y_t, t)$  and  $\sigma_0(Y_t, t)$  of the spot price process, which results in  $\{Z_t(\hat{\Theta})\}$  being more inclined to follow i.i.d.  $U[0, 1]$  and thus obtaining a lower  $Q(j)$ . Based on the above inference, a superior model specification of an SV model can also be identified according to its lower  $Q(j)$  calculated based on  $\{Y_t = \ln(S_t)\}$ .

## Funding

The authors thank the Ministry of Science and Technology of Taiwan for financial support.

## Conflict of interest statement

We would like to thank the editor and two anonymous referees for their valuable comments and suggestions. All errors are our own.

## References

- Ahn, D., and B. Gao. 1999. A Parametric Nonlinear Model of Term Structure Dynamics. *Review of Financial Studies* 12: 721–762.
- Ait-Sahalia, Y. 1996. Testing Continuous-Time Models of the Spot Interest Rate. *Review of Financial Studies* 9: 385–426.
- Ait-Sahalia, Y., and R. Kimmel. 2007. Maximum Likelihood Estimation of Stochastic Volatility Models. *Journal of Financial Economics* 83: 413–452.
- Andersen, T. G., T. Bollerslev, and N. Meddahi. 2005. Correcting the Errors: Volatility Forecast Evaluation Using High-Frequency Data and Realized Volatilities. *Econometrica* 73: 279–296.
- Bakshi, G., C. Cao, and Z. Chen. 1997. Empirical Performance of Alternative Option Pricing Model. *The Journal of Finance* 52: 2003–2049.
- Bakshi, D., N. Ju, and H. Ou-Yang. 2006. Estimation of Continuous-Time Models with an Application to Equity Volatility Dynamics. *Journal of Financial Economics* 82: 227–249.
- Bates, D. 1996. Jump and Stochastic Volatility: Exchange Rate Processes Implicit in Deutsche Mark Options. *Review of Financial Studies* 9: 69–107.
- Bates, D. 2000. Post-'87 Crash Fears in the S&P 500 Futures Option Market. *Journal of Econometrics* 94: 181–238.
- Branger, N., A. Kraftschik, and C. Volkert. 2016. "The Fine Structure of Variance: Pricing VIX Derivatives in Consistent and Log-VIX Models." *Working paper, University of Muenster*.
- Broadie, M., M. Chernov, and M. Johannes. 2007. Model Specification and Risk Premia: Evidenced from Futures Options. *The Journal of Finance* 62: 1453–1490.
- Chacko, G., and L. Viceira. 2003. Spectral GMM Estimation of Continuous-Time Processes. *Journal of Econometrics* 116: 259–292.
- Chernov, M., A. R. Gallant, E. Ghysels, and G. Tauchen. 2003. Alternative Models for Stock Price Dynamics. *Journal of Econometrics* 116: 225–257.
- Chourdakis, K., and G. Dotsis. 2011. Maximum Likelihood Estimation of Non-affine Volatility Processes. *Journal of Empirical Finance* 18: 533–545.

variance, it is difficult to assess the bias or extra noise caused by this approximation; the effectiveness of the test may be influenced significantly.

- Christoffersen, P., K. Jacob, and K. Mimouni. 2010. Volatility Dynamics for the S&P 500: Evidence from Realized Volatility, Daily Returns, and Option Prices. *Review of Financial Studies* 23: 3141–3189.
- Durham, G. 2007. SV Mixture Models with Application to S&P 500 Index Returns. *Journal of Financial Economics* 85: 822–856.
- Durham, G. 2013. Risk-Neutral Modeling with Affine and Nonaffine Models. *Journal of Financial Econometrics* 11: 650–681.
- Duan, J., and C. Yeh. 2010. Jump and Volatility Risk Premiums Implied by VIX. *Journal of Economic Dynamics and Control* 34: 2232–2244.
- Duffie, D., J. Pan, and K. Singleton. 2000. Transform Analysis and Asset Pricing for Affine Jump-Diffusions. *Econometrica* 68: 1343–1376.
- Eraker, B. 2004. Do Equity Prices and Volatility Jump? Reconciling Evidence from Spot and Option Prices. *The Journal of Finance* 59: 1367–1403.
- Eraker, B., M. Johannes, and N. Polson. 2003. The Impact of Jumps in Volatility and Returns. *The Journal of Finance* 58: 1269–1300.
- Ferriani, F., and S. Pastorello. 2012. Estimating and Testing Non-affine Option Pricing Models with a Large Unbalanced Panel of Options. *The Econometrics Journal* 15: 171–203.
- Heston, S. 1993. A Closed-Form Solution for Options with Stochastic Volatility with Applications to Bond and Currency Options. *Review of Financial Studies* 6: 327–343.
- Hong, Y., and H. Li. 2005. Nonparametric Specification Testing for Continuous-Time Models with Applications to Term Structure of Interest Rates. *Review of Financial Studies* 18: 37–84.
- Ignatieva, K., P. Rodrigues, and N. Seeger. 2015. Empirical Analysis of Affine versus Nonaffine Variance Specifications in Jump-Diffusion Models for Equity Indices. *Journal of Business & Economic Statistics* 33: 68–75.
- Jones, C. 2003. The Dynamics of Stochastic Volatility: Evidence from Underlying and Options Markets. *Journal of Econometrics* 116: 181–224.
- Kaeck, A., and C. Alexander. 2012. Volatility Dynamics for the S&P 500: Further Evidence from Non-affine, Multi-factor Jump Diffusions. *Journal of Banking & Finance* 36: 3110–3121.
- Li, M. 2010. A Damped Diffusion Framework for Financial Modeling and Closed-Form Maximum Likelihood Estimation. *Journal of Economic Dynamics and Control* 34: 132–157.
- Lo, C.-L., P.-T. Shih, Y.-W. Wang, and M.-T. Yu. 2019. VIX Derivatives: Valuation Models and Empirical Evidence. *Pacific-Basin Finance Journal* 53: 1–21.
- Malik, S., and M. Pitt. 2011. Particle Filters for Continuous Likelihood Evaluation and Maximisation. *Journal of Econometrics* 165: 190–209.
- Mijatovic, A., and P. Schneider. 2014. Empirical Asset Pricing with Nonlinear Risk Premia. *Journal of Financial Econometrics* 12: 479–506.
- Newey, W. K., and K. D. West. 1987. A Simple, Positive Semi-Definite, Heteroskedasticity and Autocorrelation Consistent Covariance Matrix. *Econometrica* 55: 703–708.
- Pan, J. 2002. The Jump-Risk Premia Implicit in Options: Evidence from an Integrated Time-Series Study. *Journal of Financial Economics* 63: 3–50.